AerospaceEurope Conference2021
WARSAW, POLAND | 23 -26 NOVEMBER 2021
PSAA
CEAS Council of European Aerospace Societies

PRELIMINARY DESIGN OF AIRCRAFT WINGS INCORPORATING FOLDING WINGTIPS

Huaiyuan Gu , Fintan Healy & Jonathan Cooper

Dept of Aerospace Engineering, University of Bristol, Bristol, BS8 1TR UK

Abstract

There is a great drive currently towards reducing the environmental impact of aircraft and one concept that is receiving much interest are designs with much higher aspect ratios (HAR) wings. Recent work has shown that folding wingtip configurations, which are necessary for aircraft with a large wingspan to fit into airport gate limits, can be used as a means to (i) facilitate loads alleviation and thus enabling better aerodynamic performance without the corresponding weight increase; (ii) improve roll performance. This work considers how HAR wings incorporating floating folding wingtips can be included in the preliminary design phase. A baseline A321-like configuration is compared to an AR-19 planform with different sizes of folding wingtip. It is shown that the use of floating folding wingtips can reduce the aircraft weight by up to 25%, leading to around a 10% improvement in range.

Keywords: high aspect ratio wings, folding wingtips, semi-aeroelastic hinge, preliminary aircraft design

1. Introduction

The growing demand for fuel-efficient and environmentally friendly aircraft calls for a step-change in the aerodynamic performance of modern civil aircraft combined with a reduction in structural weight and more efficient propulsion. This pressing need has been identified by research programs across the world such as the ICAO, FLIGHTPATH2050 [1] and CLEANSKY2 [2] initiatives, with challenging goals set for reductions in CO2, NOx and noise by the year 2050. Using high aspect ratio wings is particularly of interest to aircraft designers due to the inherent reduction in induced drag, leading to a tremendous improvement in the lift-to-drag ratio (L/D). However, there are a number of challenges in practice. Chief among these is the limitations on the wingspan imposed by airport operational requirements such as gate limits, runway and taxi-way separation. Therefore, incorporating folding wingtip devices on high aspect ratio wings has become one of the most attractive solutions, as such a device would allow the wingtip to fold up on the ground, enabling the aircraft to meet operational requirements.

Calderon et.al[3] performed sizing studies on aircraft numerical models with a range of wing aspect ratios (AR), and concluded that the optimum aspect ratio lies between 18 to 19, as shown in Figure 1, significantly higher than that used in current aircraft designs. When the AR increased above 20, a dramatic reduction in the predicted range was seen due to the increased structural weight of the wing resulting from the increase in bending moments. Recent studies have considered the use of flared folding wingtip devices incorporating a semi-aeroelastic hinge i.e. a hinge mechanism that can be actively released in flight, as a load alleviation device, to mitigate the increased bending loads [4–6]. With the hinge line rotated outboard with respect to the incoming flow, as shown in Figure 2, the local angle of attack on the folding wingtip reduces with the fold angle, θ. When the hinge is released in flight, the wingtip folds towards a stable condition at a particular fold angle, known as the coast angle, about which the aerodynamic and gravitational moments about the hinge balance and the system is statically stable. The influence of the flare angle and hinge stiffness on the load alleviation has been investigated [5]. where it has been shown that improved load alleviation can be obtained by increasing the flare angle, Λ, and reducing the hinge stiffness. It should also be noted that the floating folding wing tips passively enhance the roll performance [7] but this effect is not considered in this work.

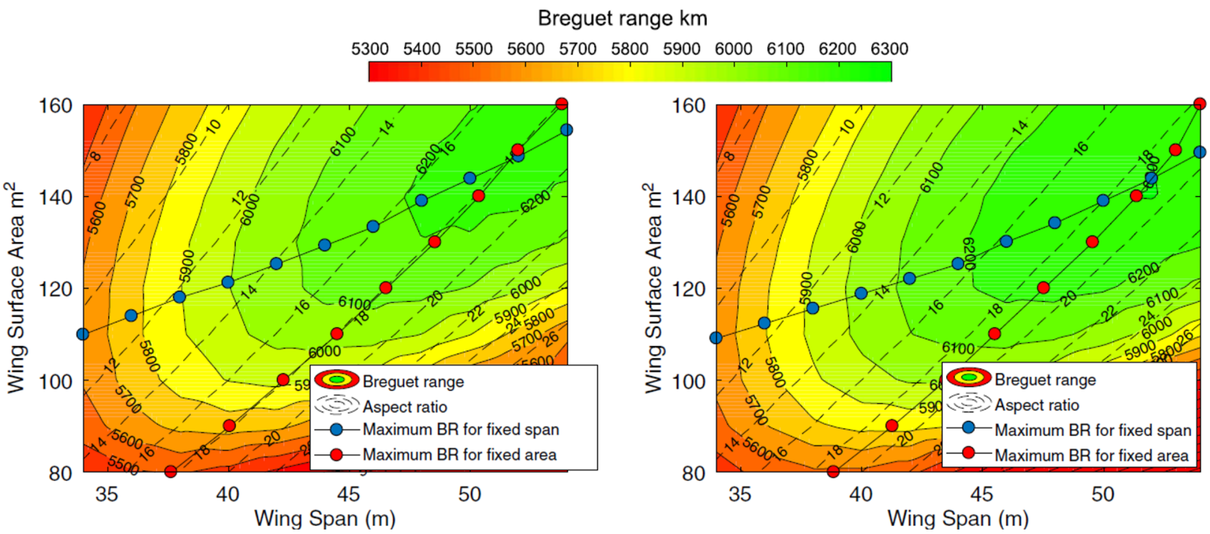

Figure 1 – Parametric sweep of the wing surface area and wingspan [3].

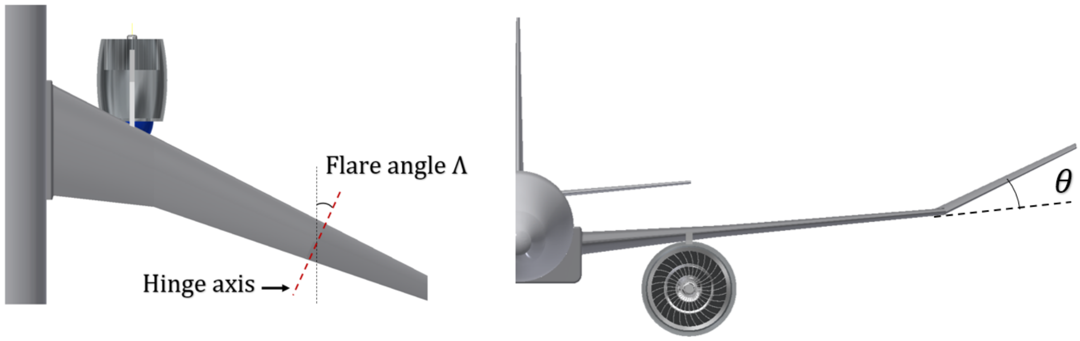

Figure 2 – Schematic drawing of the folding wing tip with a positive flare angle, Λ, [5].

In this work, sizing (determining the minimum size of the internal structure that meets all constraints) is performed on aircraft models created with high aspect ratio wings incorporating various folding wingtip configurations. The details of the aeroelastic models are described in section 2 including the planform geometry, structural and aerodynamic models. Section 3 presents the sizing framework which was established for the preliminary design of new wing configurations including folding wingtips and semi-aeroelastic hinges. Finally, the calculated wing weights are used to predict the range of aircraft according to the Breguet range equation. The results help to provide insight into the benefits of using the folding wingtip as a load alleviation device at the overall system level.

2. Aircraft model

An A321-like model was chosen as the baseline model, where the details of the planform geometry and mass configurations were listed in Table 1. Then, an aircraft model that incorporated floating wing-tips in a configuration with aspect ratio of 19 was created by stretching the wingspan of the baseline model. During this process, the wing surface area, leading-edge sweep angle, taper ratio and engine position were kept constant, as illustrated in Figure 4. Figure 5 shows the aeroelastic model used in the analysis, where the airframe is modelled using beam elements (element code CBEAM in Nastran) and the material properties were assumed to be Aluminium 7075 with modulus and yield strength of 70 GPa and 520 MPa respectively. The payload, fuel mass and system weight were modelled using distributing lumped masses across the airframe (element code CONM2 in Nastran). The Aerodynamic forces were computed using the Double Lattice Method (DLM) implemented in MSC. Nastran. A beam spline was defined to generate coupling between the aerodynamic mesh and the structural nodes, allowing for the aerodynamic forces to be transferred to the airframe and change with respect to the displacement of the structural nodes. Note that the aerodynamic panels were only assigned to the wings and tailplane; the aerodynamic forces produced by the fuselage and engine nacelles were neglected.

A folding wingtip was implemented on this new wing configuration, which was modelled as a separate body, with the relative motion of the inner wing and wingtip constrained at two coincident nodes along the hinge line, only allowing for the relative rotation about the hinge line as shown in Figure 6. The so-called semi aeroelastic hinge (SAH) [5] was implemented on each wing, which is locked during cruise to obtain the optimum aerodynamic efficiency, and then released during manoeuvres or severe gusts to reduce the loads carried by the wing.

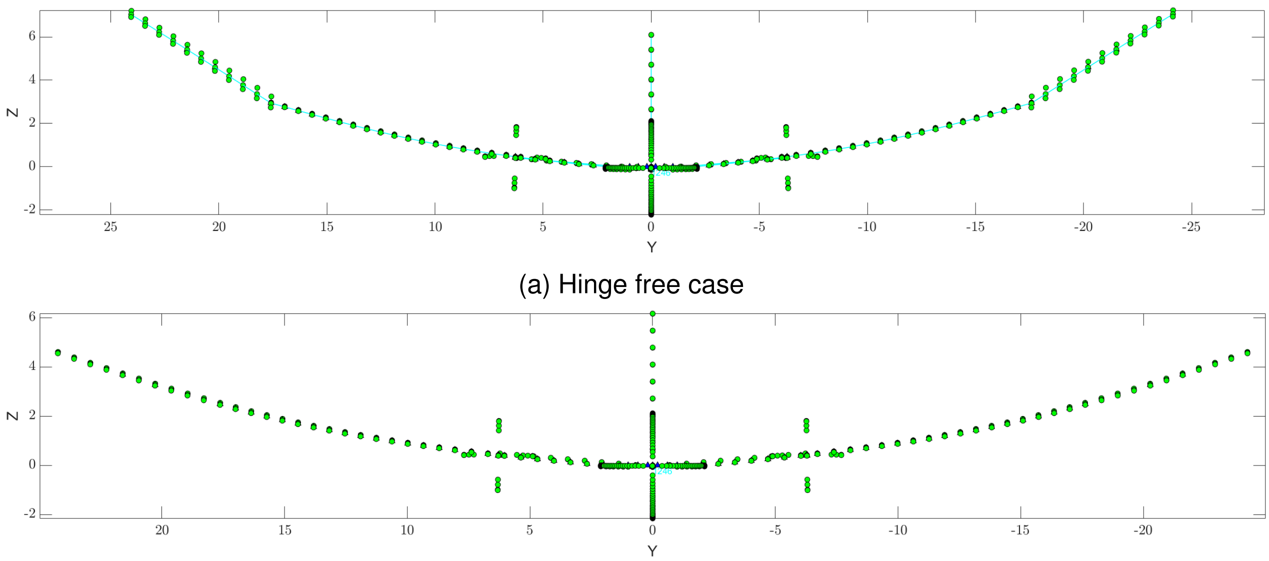

(a) Hinge free case

(b) Hinge locked case

Figure 3 – Wing deformation of the new wing configuration with folding wingtip size $\eta = 30\%$ during (a)manoeuvres and gust encounters (b)cruise

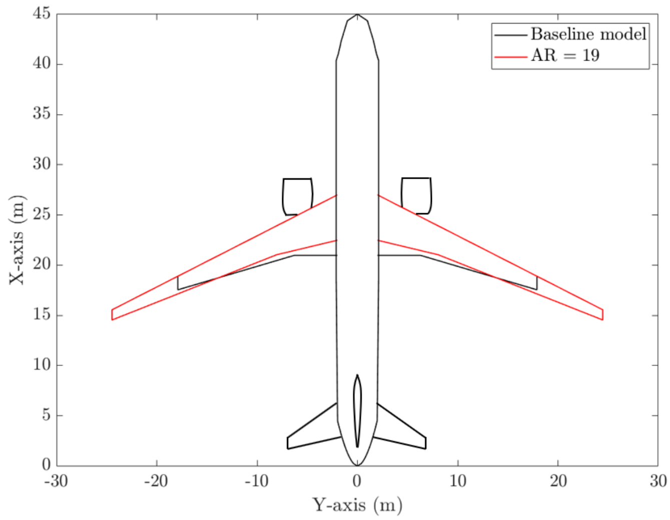

Figure 4 – Comparison of the new wing planform with increased aspect ratio to that of the baseline model.

Table 1 – Summary of the baseline aircraft model (A321).

Wing plan form Parameters	**Values**		
Span position(m)	2	6.37	17.5
LE sweep angle(°)	0	27	27
TE sweep angle(°)	0	0	16.5
Dihedral(°)	0	5	5
Thickness ratio	0.15	0.12	0.11
Front spar	0.15	0.15	0.15
Rear spar	0.65	0.65	0.65
Mass configurations	**Mass (kg)**		
Payload	25000		
Max.take off weight (MTOW)	97000		
Operating weight empty (OWE)	47800		
Max. fuel weight	25860		
Engine mass	7362		
Pylon	1630		

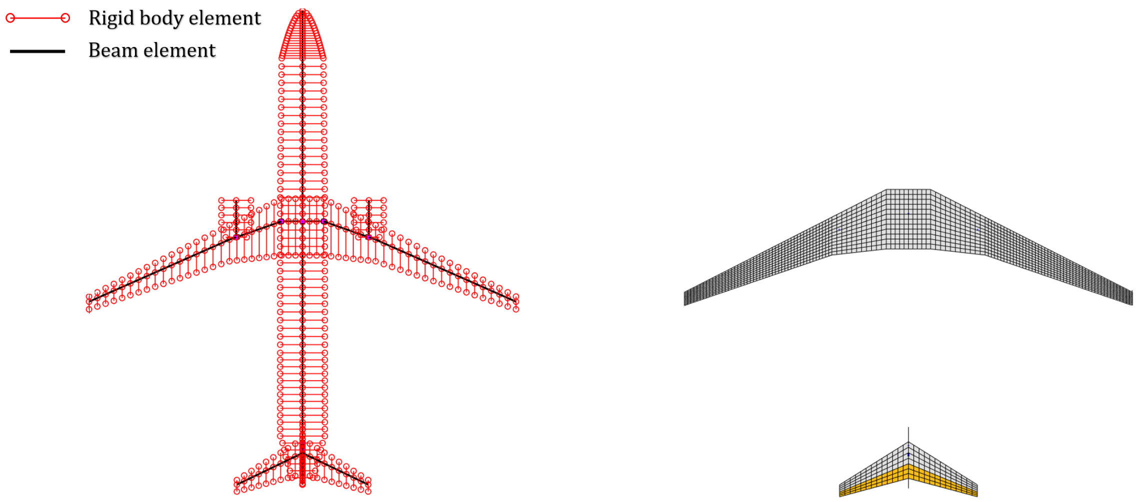

(a) structural model (b) aerodynamic model

Figure 5 – Aeroelastic model used in the analysis

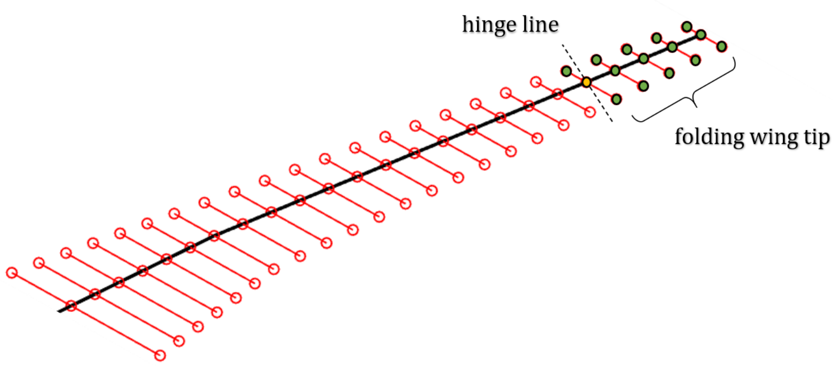

Figure 6 – Structural model of the wing with folding wingtip.

3. Sizing framework

This section describes the sizing framework that was established to perform preliminary design of the wing configuration incorporating folding wingtips and semi-aeroelastic hinges, as shown in Figure 8. The mass configuration was assumed to be identical to that of the baseline model as given in Table 1, and the maximum take-off mass was used to estimate the secondary structural mass of the wing such as the high-lifting devices on the leading and trailing edge using the empirical formulae proposed in the work of Torenbeek[8]. The hinge weight was taken to have a mass of 200 kg on each wing. The wing structure was assumed to be a box-beam as shown in Figure 7, where the stiffness and strength were determined by the thickness of individual components i.e. spar cap, web and skin-stringer panel. For each sizing iteration, the optimisation of the aerodynamic twist was performed (jig twist optimisation) to ensure an elliptical lift distribution was achieved along the wingspan during cruise to maximise the aerodynamic efficiency.

On each design iteration aerodynamic loads were computed at a range of load cases including both static manoeuvres and gust encounters, as shown in Table 2. The worst case calculated loads were then used for structural sizing. The spar caps were sized to withstand the bending loads i.e. the thickness was calculated to avoid tensile yield and column buckling. The web thickness was determined by the shear flow contributed from the vertical shear force and torque. The dimensions of the skin-stringer panel, including skin thickness, stringer pitch, thickness and width of individual stringer segments were sized based on the external bending loads, following the design guidelines proposed in the work of Niu[9]. The structural properties including the bending and torsional stiffness were updated based on the calculated component thickness prior to the next sizing iteration. The whole iterative process was terminated when the thickness of individual components converged, at which time a safety factor of 1.5 was applied throughout the sizing process.

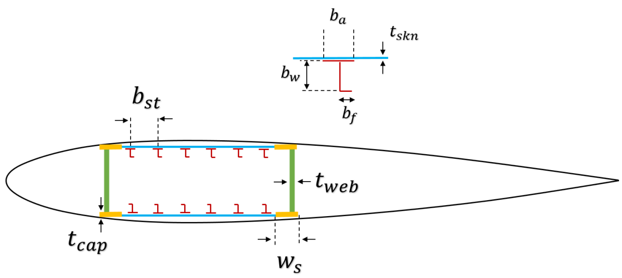

Figure 7 – Cross section of the wing-box used for sizing.

Table 2 shows the load cases considered in the sizing framework. Load cases 1-3 were considered with the aircraft manoeuvring at different altitudes where the hinge is released. Load cases 4-6 evaluate gust responses of the aircraft with free hinge wingtips. In this study, the aircraft is assumed to be subjected to a family of discrete gusts in the form of one minus cosine (1MC) gusts [10]. The gust length, L_g, ranges from 18 to 214 metres according to CS-25 certification specifications [11] and the gust profile is defined as

$$w_g(t) = \frac{U_{ds}}{2}(1-\cos\frac{2\pi Vt}{L_g}) \tag{1}$$

where V is the true air speed (TAS) and U_{ds} is the peak gust velocity, which is calculated as

$$U_{ds} = U_{ref}F_g(\frac{H}{106.17})^{\frac{1}{6}} \tag{2}$$

F_g is the load alleviation factor which is taken here as 1. U_{ref} is the reference gust velocity determined based on the CS-25 certification specifications, which varies linearly from 13.4 m/s at an altitude of 15,000 ft to 7.9 m/s at an altitude of 50,000 ft. Load case 7 represents the cruising condition with small gust encounters, where the hinge is locked. A gust threshold is defined that the SAH will only be unlocked when the gust load reaches above 30% of the worst-case gust load at the corresponding altitude. The hinge jammed case is considered in load case 8, i.e. the hinge is locked during gust encounters; however, in this specific load case the safety factor is set as 1 instead of 1.5 to account for the reduced probability of this failure case occurring.

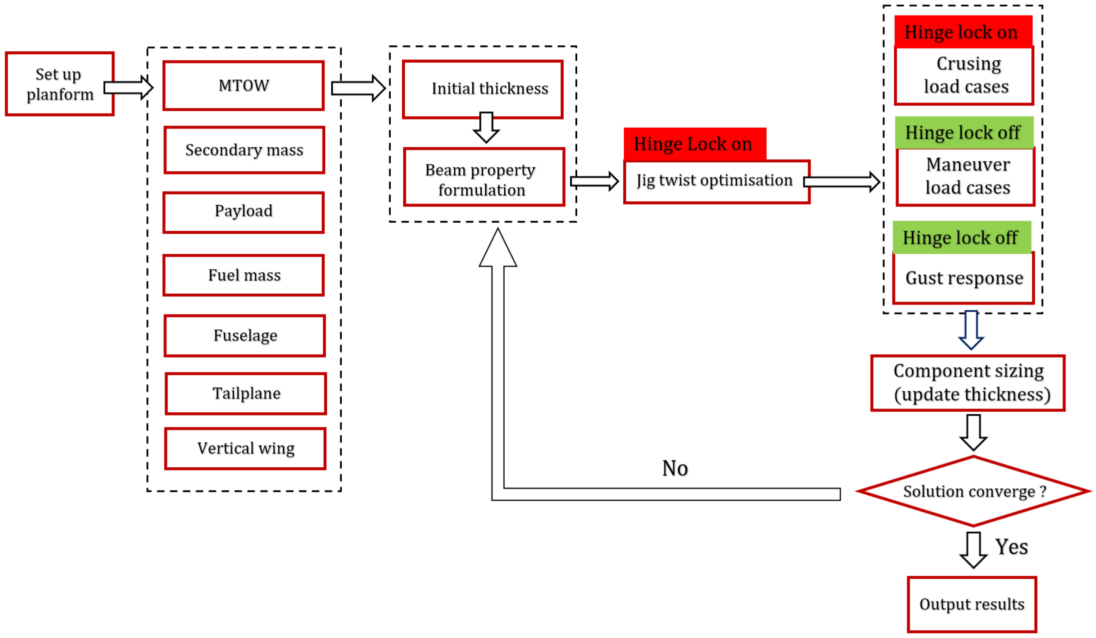

Figure 8 – Sizing framework for the wing configuration incorporating a semi-aeroelastic hinge.

Table 2 – Load cases considered in the sizing.

Load case	Load factor (g)	Gust length (m)	Gust peak	Mach No.	Altitude (ft)	Hinge
1	2.5	NA	NA	0.78	36000	free
2	2.5	NA	NA	0.48	3000	free
3	-1	NA	NA	0.48	3000	free
4	1	18–214	w_g	0.78	36000	free
5	1	18–214	w_g	0.6	20000	free
6	1	18–214	w_g	0.48	3000	free
7	1	18–214	Threshold	0.78	36000	locked
8	1	18–214	w_g $(S.F. = 1)$	0.48	3000	locked

4. Results

Figure 9 shows the distributions of the worst-case loads including the out of plane bending moment, vertical shear force and torque occurring along the wing during manoeuvre and cruise conditions. It shows that the bending moment reduces significantly with the increasing size of the folding wingtip, η, particularly at the wing root. An obvious reduction in the shear force is also seen along the wingspan, whereas the variation at the wing root is relatively small. There is no clear relationship between the folding wingtip size, η, and the observed torque distributions from the results. The black dashed curves shown in Figure 9 represent the external loads occurred during cruise which was found to be insensitive to the change of η.

Figure 10 shows the overall weight of the wing incorporating various folding wingtip sizes, η. For the hinge locked case, the wing weight was 12,100 kg, 60$\%$ higher than that of the baseline model. However, a significant reduction in the wing weight was achieved by incorporating the semi-aeroelastic hinge, due to its load alleviation capability as shown in Figure 9, albeit with a small weight penalty caused by the hinge mass. Note that it has been assumed that the hinge mass doesn't change with wingtip size, although in practice it probably would. The wing weight reduces with increasing folding wingtip size, η, and approximately a 25 $\%$ reduction in the wing weight was achieved when $\eta = 40\%$.

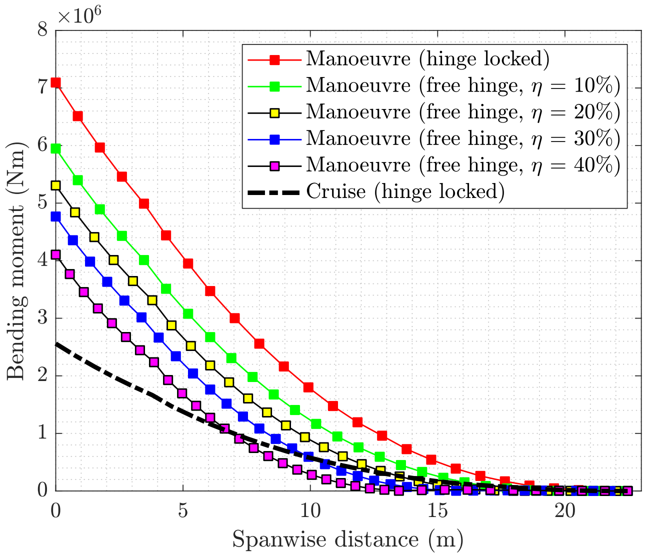

(a)

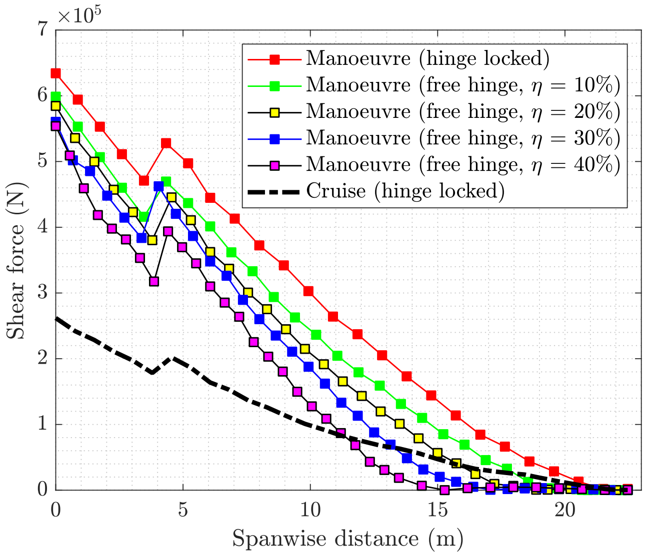

(b)

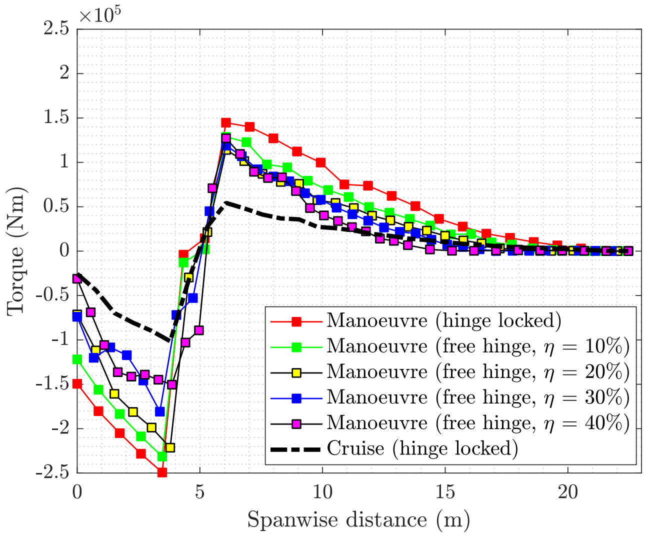

(c)

Figure 9 – The distributions of external loads occurring on the wing during manoeuvres and cruise.

Figure 11 compares the drag polar of the AR19 configuration and the baseline model. The induced drag was estimated based upon the lift distribution where the detailed computation is established in the work of Kalman et.al. [12]. The zero-lift drag was estimated by summing up the contributions of individual components including the fuselage, wings, and nacelle [13]. A dramatic reduction in induced drag was achieved in the new configuration compared to the baseline model due to the increase in the wing aspect ratio. The Breguet range equation was used to estimate the range of the aircraft models[14]

$$Range = \frac{V}{SFC\ g}\frac{L}{D}\ln(\frac{W_i}{W_f}) \tag{3}$$

where the specific fuel consumption, SFC, is taken as 16.03 $(g/s)/kN$, V is the cruise speed which is assumed to be 0.78 Mach, W_i and W_f are the initial and final weight of the aircraft. The mission was set for half payload (12,500 kg) and half fuel tank (12,930 kg), and the calculated ranges are shown in Figure 12. For the hinge locked case, approximately 10% improvement in range was obtained in the new configuration compared to that of the baseline model. Higher improvements were achieved by increasing the size of the folding wingtip, η with an additional 4% gain in range seen for $\eta = 40\%$.

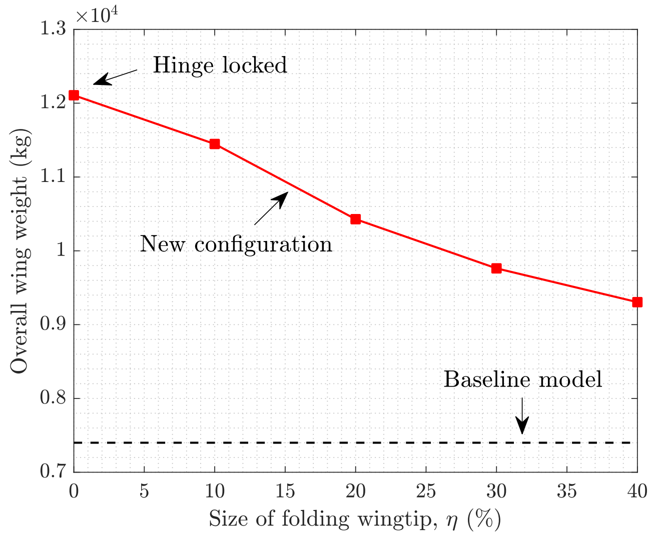

Figure 10 – Wing weight of the baseline model and new configuration incorporating folding wingtips with various sizes, η.

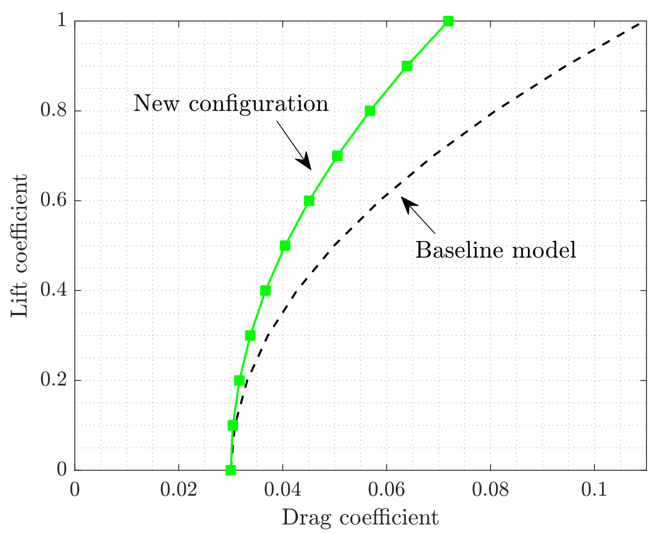

Figure 11 – Comparison of drag polar between the new configuration and the baseline model.

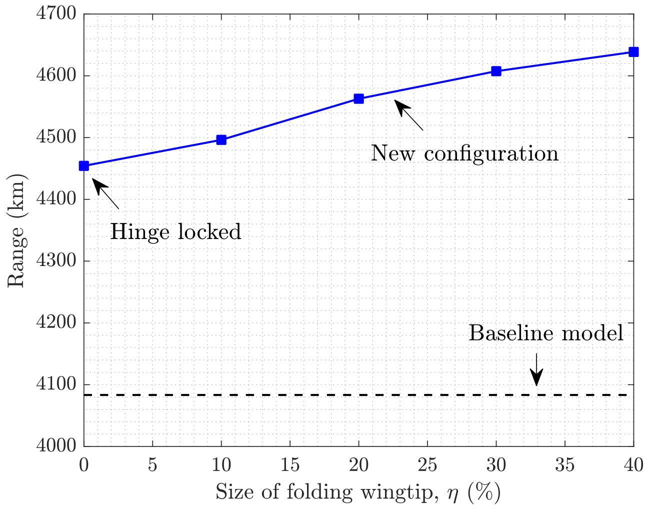

Figure 12 – Comparison of predicted ranges of the aircraft models.

5. Concluding remarks

In this paper, structural sizing was performed on the aircraft models designed with high aspect ratio wings incorporating folding wingtip devices. The influence of using folding wingtips as a load alleviation device on the wing weight and aircraft range was examined. It is found that the bending moment on the wing can be significantly mitigated by increasing the size of the folding wingtips, η, leading to reduced structural weight. A reduction in the wing weight of more than 25% was observed for $\eta = 40\%$. Around a 10 % increase in range, calculated using the Breguet range equation, was seen when the wing aspect ratio increased from 10 to 19, with a further 4% additional improvement achieved by increasing the size of folding wingtips. Current results suggested that the increase in the folding wingtip size is beneficial for aircraft performance. However, the current design framework needs to be enhanced to take into account more sophisticated modelling techniques, including structural and aerodynamic non-linearities, stability considerations such as flutter analysis and also the implementation of the folding mechanism, to verify the conclusions and determine the optimum folding wingtip design.

6. Acknowledgments

This work was performed as part of the U-HARWARD (Ultra High Aspect Ratio Wing Advanced Research and Designs) project which has received funding from the European Union's Clean Sky 2 research programme under grant agreement No 886552. The second author is supported by the Engineering and Physical Science Research Council (EPSRC) iCASE award (19000004) sponsored by Airbus Operations UK Ltd..

7. Contact Author Email Address

Professor J.E.Cooper Email: j.e.cooper@bristol.ac.uk

8. Copyright Statement

References

[1] Strategic research and innovation agenda (sria) 2017 update,. *Advisory Council for Aviation Research and Innovation in Europe*, 2017.

[2] Consolidated annual activity report. *Clean Sky 2 Joint Undertaking*, 2019.

[3] D. E. Calderon, J. E. Cooper, M. Lowenberg, S. A. Neild, and E. B. Coetzee. Sizing high-aspect-ratio wings with a geometrically nonlinear beam model. *Journal of Aircraft*, 56(4):1455–1470, 2019.

[4] A. Castrichini, V. Hodigere Siddaramaiah, D. E. Calderon, J. E. Cooper, T. Wilson, and Y. Lemmens. Nonlinear folding wing tips for gust loads alleviation. *Journal of Aircraft*, 53(5):1391–1399, 2016.

[5] A. Castrichini, V. Hodigere Siddaramaiah, D.E. Calderon, J.E. Cooper, T. Wilson, and Y. Lemmens. Preliminary investigation of use of flexible folding wing tips for static and dynamic load alleviation. *The Aeronautical Journal*, 121(1235):73–94, 2017.

[6] Cheung. R. C. M., Rezgui. D., J. E. Cooper, and Wilson. T. Testing of a hinged wingtip device for gust loads alleviation. *Journal of Aircraft*, 55(5):2050–2067, 2018.

[7] Fintan Healy, Ronald C. Cheung, Theodor Neofet, Mark H. Lowenberg, Djamel Rezgui, Jonathan E. Cooper, Andrea Castrichini, and Tom Wilson. Folding wingtips for improved roll performance. *Journal of Aircraft*, 2021.

[8] E. Torenbeek. Development and application of a comprehensive, design-sensitive weight prediction method for wing structures of transport category aircraft. *Delft Univ. of Technology Rept*, 1992.

[9] Michael C. Niu. *Airframe Stress Analysis and Sizing*. Adaso/Adastra Engineering Center, 3^{rd} edition, 2011.

[10] J. R. Wright and J. E. Cooper. Introduction to aircraft aeroelasticity and loads 2nd edition. *John Wiley & Sons*, 2014.

[11] Cs-25 certification specifications for large aeroplanes. *European Aviation Safety Agency (EASA)*, 2003.

[12] Kalman. T. P., Giesing. J. P., and Rodden. W. P. Spanwise distribution of induced drag in subsonic flow by the vortex lattice method. *Journal of Aircraft*, 7(6):574–576, 1970.

[13] Daniel P. Raymer. *Aircraft Design: A Conceptual Approach*. AIAA Education Series, 5^{th} edition, 2012.

[14] Darren Rhodes Lloyd R Jenkinson, Paul Simpkin. *Civil jet aircraft design*. Butterworth-Heinemann, 1999.